Final Report of NASA Research Grant

entitled

BIDIRECTIONAL REFLECTANCE MODELING OF NON-HOMOGENEOUS PLANT CANOPIES

Principal Invesigator

John M. Norman
Department of Agronomy
203 KCR Building
University of Nebraska
Lincoln, NE 68583-0817

September 16, 1987 - September 15, 1986

Grant # NAG 5-277

BIDIRECTIONAL REFLECTANCE MODELING OF NON-HOMOGENEOUS PLANT CANOPIES

John M. Norman
University of Nebraska
Lincoln, NE 68583

Objective

The objective of this research is to develop a 3-dimensional radiative transfer model for predicting the bidirectional reflectance distribution function (BRDF) for heterogeneous vegetation canopies. The model (named BIGAR) considers the angular distribution of leaves, leaf area index, the location and size of individual subcanopies such as widely spaced rows or trees, spectral and directional properties of leaves, multiple scattering, solar position and sky condition, and characteristics of the soil. The model relates canopy biophysical attributes to down-looking radiation measurements for nadir and off-nadir viewing angles. Therefore inversion of this model, which is difficult but practical, should provide surface biophysical properties from radiation meaurements for nearly any kind of vegetation pattern; a fundamental goal of remote sensing. Such a model also will help to evaluate atmospheric limitations to satellite remote sensing by providing a good surface boundary condition for many different kinds of canopies. Further this model can relate estimates to nadir reflectance, which is approximated by most satellites, to hemisphereical reflectance, which is necessary in the energy budget of vegetated surfaces.

Technical Approach

The approach to this research requires development of the mathematical equations and computer coding of the heterogeneous-canopy model, better characterization of leaf and soil properties which are a serious limitation at the present time, and finally comparison of model predictions with field measurements that are obtained from other investigators. The Bidirectional General Array Model (BIGAR) is based on the concept that heterogeneous canpies can be described by a combination of many subcanopies, which contain all the foliage, and these subcanopy envelopes can be characterized by ellipsoids of various sizes and shapes. The foliage within an ellipsoid may be randomly positioned or non-randomly positioned. Estimates of multiple scattering are obtained by transforming each point of interest in a particular ellipsoidal canopy to an equavalent one-dimensional canopy and solving the radiative transfer equations for this simple case. The BRDF for individual leaves has been measured so that appropriate leaf properties can be used in the model. The BRDF for several soils has been measured and modeled with a simple block-modeling approach to provide a reasonable lower boundary condition for the canopy model. Field measurements of corn and soybean canopy BRDFs are compared with model predictions.

Research Results

The results from this grant research are four fold: 1) Measurement of leaf bidirectional reflectance and transmittence distribution functions, 2) development and testing of three-dimensional model (BIGAR) with measurements from corn and soybean, 3) development and testing of two simple soil bidirectional reflectance models.

The measurements of leaf bidirectional reflectance and transmittance distribution are published in Walter-Shea (1987). A journal paper is in the final stage of preparation and Appendix A contains an abstract of the leaf measurement work.

The three-dimensional, bidirectional reflectance model was developed under this grant and tested on data from the Laboratory for Applications to Remote Sensing. The Ph.D. thesis arising from this research is still in preparation so a brief model description is included in Appendix B.

Two soil bidirectional reflectance models have been developed: One represents soil particles as rectangular blocks (Norman et al., 1985) and the second represents soil particles as spheres. The sphere model is superior as seen from the results presented in Appendix C, which is a puliminary draft of a paper on soil bidirectional reflectance.

Significance of the Results

The comparisons between the BIGAR model and measurements indicate that this relatively simple model captures the essential character of row crop bidirectional reflectance distribution functions. The results from the soil BRDF models indicates that the two-parameter, sphere soil model provides an excellent representation of the soil BRDF. This will aid in establishing a simple way to define the soil boundary condition for any canopy-plus-soil BRDF model.

The measurements of leaf bidirectional reflectance and transmittance distribution functions are the first such complete measurements. They clearly show that leaves are complex scatterers and condierable specular reflectance is possible from leaves. Because of the character of leaf reflectance, true leaf reflectance is larger than the nadir reflectances that normally are used to represent leaves.

Future Work

Future research should emphasize the inversion of 3-dimensional vegetation-soil bidirectional flectance factor models and develop simpler direction and wavelength information should be combined in the inversion process to extract the maximum amount of information; perhaps inverting the distribution of normalized-difference with view angle may hold promise. The logical extension of this 3-D is to include more complex canopy architecture such as conifer trees, and also extend the wavelength band to the thermal.

BIDIRECTIONAL REFLECTANCE MODELING OF NON-HOMOGENEOUS PLANT CANOPIES

John M. Norman
University of Nebraska
Lincoln, NE 68583

Publications

Norman, J. M. and J. W. Welles. 1983. Radiative transfer in an array of canopies. Agron. J. 75:481-488.

Walthall, C. L., J. M. Norman, J. M. Welles, G. Campbell and B. L. Blad. 1985. A simple equation to approximate the bidirectional reflectance from vegetated surfaces. Appl. Optic 24:383-387.

Norman, J. M., J. M. Welles and E. A. Walter. 1985. Contrasts among bidirectional reflectance of leaves, canopies and soils. IEEE Trans. GeoSci. Remote Sensing, GE-23:659-667.

Kimes, D. S., J. M. Norman and C. L. Walthall. 1985. Modeling the radiant transfers of sparse vegetation canopies. IEEE Trans. GeoSci. Remote Sensing, GE-23:695-704.

Norman, J. M., J. Specht, B. L. Blad and J. M. Welles. 1982. The effect of pubescence on soybean leaf and canopy reflectance. Amer. Soc. Agron. Abstracts. Madison, WI 53706. p. 17.

Norman, J. M. 1984. Using canopy reflectance properties to estimate some parameters essential to macroscale Et predictions. Amer. Geophys. Union Abstracts, Fall, 1985. AGU, Washington, D. C.

Norman, J. M., J. M. Welles, E. A. Walter and G. S. Campbell. 1984. A bidirectional reflectance model for heterogeneous plant canopies. Amer. Soc. Agron. Abstracts, Madison, WI 53706. p. 15.

Walter, E. A., J. M. Norman, J. M. Welles and B. L. Blad. 1984. Leaf bidirectional reflectance measurements in corn and soybean. Amer. Soc. Agron. Abstracts, Madison, WI 53706. p. 19.

Walter-Shea, E. A. 1987. Laboratory and field measurements of leaf spectal properties and canopy architecture and their effects on canopy reflectance. Ph.D. Thesis, Univ. of Nebraska, Lincoln, NE. 201 pp.

Presentations

1982 Volunteer paper - The effect of pubescence on soybean leaf and canopy reflectance. Amer. Soc. Agron. Annual Meeting, Anaheim, CA, Nov. 28-Dec. 3.

1984 Invited paper - Using canopy reflectance properties to estimate some parameters essential to macroscale Et predictions. Hydrology Symposium on Evapotranspiration Modeling, Fall Amer. Geophys. Union Meeting, San Francisco, CA, Dec. 3-7.

1984 Volunteer paper - A bidirectional reflectance model for heterogeneous plant canopies. Amer. Soc. Agron. Annual Meeting, Las Vegas, NE, Nov. 25-30.

1984 Invited to present research results at Fundamental Research Project Briefing at NASA Headquarters for Dr. Shelby Tilford and Dr. Burton Edelson, Washington, D. C. Mar. 16.

1984 Invited seminar - Bidirectional reflectance in heterogeneous plant canopies. Monthly seminar series jointly sponsored by U. of Maryland RSSL and NaSA/GSFC, Washington, D. C. July 19.

1986 Invited Paper - Synthesis of Canopy Processes. Seminar Series Symposium of the British Society for Experimental Biology, Univ. of Nottingham, England, Mar. 25-27, 1986.

1986 Invited Presentation - Radiative Transfer and Spectral Signature of Plant Canopies. Workshop on Climate-Vegetation Interactions, Sponsored by NASA, Jan. 17-19, 1986.

APPENDIX A

Abstract of Chapter 2 from

Walter-Shea, E. A. 1987. Laboratory and Field Measurements of Leaf Spectal Properties and Canopy Architecture and Their Effects on Canopy Reflectance. Ph.D. Thesis, Univ. of Nebraska, Lincoln, NE. 201 pp.

CHAPTER 2

LEAF BIDIRECTIONAL FLECTANCE AND TRANSMITTANCE IN CORN AND SOYBEAN

ABSTRACT

Leaves dominate the reflection of radiation from vegetative canopies. Many canopy radiative transfer models assume that leaves approximate ideal diffusers. Clearly, the directional spectral properties of leaves must be adequately characterized to make such models comprehensive and reliably predictive. Directional reflectance and transmittance factors of individual corn (Zea mays, L.) and soybean (Glycine max, Merr.) leaves were measured by employing three source incidence angles and many view angles in visible and near-infrared wavelength bands in the laboratory to characterize leaf spectral properties. Spectral distributions were characterized and hemispherical reflectance and transmittance values were computed. Forward scattering (when the viewing sensor is directed toward the source) was found to be a prominent feature with increasing source incidence angle. Hemispherical reflectance generally increased with increased incidence angle while transmittance values decreased. For example, visible reflectance for a corn leaf increased from 8.3% to 11.9%, while visible transmittance decreased from 2.8% to 2.1% (20° and 70° source incidence angles, respectively). At most source incidence angles, hemispherical reflectance factors were higher than the nadir-viewed reflectance component while hemispherical transmittances were lower. The distribution of directional reflectance changed with increasing incidence angle, with a peak in reflectance in the principal plane becoming prominent at an incidence angle of 70°. This peak was attributed to non-Lambertian reflectance. The non-Lambertian component was significant, contributing at a 70° source incidence angle to as much as 40% and 48% of total visible reflectance in corn and soybean, respectively. Characterization of bidirectional reflectance and transmittance of individual leaves should be most useful in mathematically representing non-Lambertian leaf properties in radiation transfer models.

APPENDIX B

Summary of three-dimensional model development and tests. A Ph.D. Thesis is in the final stages of preparation.

Welles, J. M. 1988. A Bidirectional Reflectance Model for Non-Random Canopies. Ph.D. Thesis in preparation, Univ. of Nebraska, Lincoln, NE.

A Bidirectional Reflectance Model for Non-random Canopies

J. M. Welles and J. M. Norman

ABSTRACT

The general array model (GAR) of Norman and Welles (1983) is extended to calculate bidirectional reflectance (reflectance as a function of angle of view and angle of illumination) of a plant stand. The new model (BIGAR) defines the plant canopy as one or more foliage-containing ellipsoids arranged in any desired pattern. Foliage within each ellipsoid can have any angle distribution, and is assumed randomly distributed, although a method of specifying sub-ellipsoids that contain foliage of varying properties is discussed. Foliage is assumed to scatter radiation in a Lambertian fashion. The soil bidirectional reflectance is modelled separately as a boundary condition. The reflectance of any given point within the plant stand is calculated from the incident radiation (diret beam, diffuse sky, and diffuse scattered from the soil and other foliage) and a view weighting factor that is based upon how much of the view is taken up by that particular point. Integrating this over a large number of grid locations provides a prediction of the bidirectional reflectance. Model predictions are compared with measurements in a soybean canopy at three stages of growth, and a corn canopy at two stages of growth.

INTRODUCTION

The brightness of a vegetative canopy as viewed from above is a function of the relative angles of the viewer and the illuminator, due to the complicated manner in which the canopy and underlying soil surface scatter the incident radiation. Canopy reflectance models provide a theoretical basis for inferences (such as crop identification, leaf area index LAI, percent ground cover, etc.) about an unknown canopy based upon measurements of its bidirectional reflectance pattern. It follows that the more general the reflectance model, the wider the range of scenes and conditions that can be analyzed for the information contained within their bidirectional reflectance distribution functions.

The bidirectional reflectance distribution function (BRDF) is computed in the model, and is the ratio of the radiance of an infinitesimal beam of radiation coming from a unit area (a function of view and illumination angles, and incident flux density) to the incident flux density on the unit area (Nicodemus et. al., (1977)). Values can range from 0 to infinity. Strictly speaking, BRDF cannot be measured directly since it is the ratio of infinitesimals. By integrating over the appropriate solid angles, the BRDF does provide a general relationship between the incident and reflected radiation. Generally, field measurements are of bidirectional reflectance factor (BRF), rather than BRDF. A BRF is the ratio of radiant flux reflected to what would have been reflected if the surface were ideal (no loss) and perfectly diffuse (lambertian). Since the reflected flux from a surface can be expressed as the product of the BRDF and the incident radiance integrated over the appropriate solid angles for source and viewer, and since the BRDF of an ideal surface is equal to 1/pi, then the bidirectional reflectance factor is simply pi times the BRDF.

BRDF's for vegetative canopies arise for a number of reasons: 1) Plants (or rows) shade other plants and the soil. This is especially important in non-uniform canopies. The view of the sunward side of an isolated bush, for example, will afford mostly sunlit leaves and sunlit soil, while a view of the opposite side will afford shaded soil and shaded leaves. Even within a uniform canopy, 2) leaves shade other leaves. The area near the anti-solar point (e.g. right near the shadow of your head) produces many sunlit leaves in the field of view, and relatively few shaded leaves. The view of the canopy looking toward the sun will provide many more shaded leaves, so the canopy will generally be darker there. 3) Foliage elements have their own BRDF and BTDF (bidirectional transmittance distribution function), and do not scatter in a Lambertian fashion. 4) The soil can have a more non-Lambertian BRDF than a vegetative canopy, so the

less soil the plant stand covers, the more important is the soil BRDF on the overall canopy reflectance. Soil BRDF's are in fact a complexity all their own, and arise from shading due to roughness, shading due to aggregate shape, and spectral and specular properties of the aggregates.

Several models have been proposed for horizontally uniform canopies. Allen et. al. (1970) used a two-flux (up and down) Kubelka-Munk (1931) theory of light scattering to predict canopy reflectance for a uniform canopy, but not as a function of view angle. This approach was also taken by Suits (1972), who specified a third flux in the direction of the viewer. Gerstl and Zardecki (1985) used a 5 layer atmospheric model coupled to a 10 layer uniform plant canopy model to analyze atmospheric influences on measured bidirectional reflectance patterns.

Since many canopies of interest are agronomic and planted by machines, row effects can be quite significant, and uniform canopy reflectance models of limited use. Verhoef and Bunnik (1976) proposed a row effect model, but the model is limited to a particular row profile, and is not extendable to conditions approaching uniform cover. Suits (1983) extended his earlier model to simulate row effects by specifying the foliage density as a function of horizontal position. Verhoef (1984) indicates an artificial angular response of the Suits model due to an assumption that all leaves are a mixture of vertical and horizontal, and goes on to describe the SAIL model, in which leaves are assumed arbitrarily inclined. Goel and Grier (1986a) also extend the Suits row model to include any general leaf angle distribution. They further specify row cross-sectional shape in terms of an ellipse, allowing realistic shape changes during a simulated growing season. Goel and Grier (1986b) describe an empirical function having 4 coefficients that describes bidirectional reflectance distributions as measured in row canopies. It should be pointed out that a number of other canopy models exist that deal with row structures (Allen (1974); Charles-Edwards and Thorpe (1976); Palmer (1977); Arkin et al. (1978); Mann et al. (1980); Whitfield (1986)), but these deal with intercepted light, and are not presented in terms of predicting reflectance as a function of view angle.

The most general approach involves modelling radiation in an individual canopy, as defined by some 3 dimensional envelope within which the foliage is contained. In principle, groups of these envelopes can then be specified in some regular array, or irregular pattern to simulate virtually any scene, such as an orchard or sparse. Charles-Edwards and Thornley (1973) describe a model of beam and diffuse light interception for an isolated canopy defined by an ellipsoid. The foliage within the ellipsoid is assumed uniformly distributed, This model is the basis for the later simulation (Charles-Edwards and Thorpe (1976)) of parallel rows of trees; the rows were "created" by extending one of the horizontal axes of the ellipse to a very long length. Mann, Curry, and Sharpe (1979) also treat the case of an individual ellipsoidal canopy, but allow for foliage density to be a function of position within the canopy. Norman and Welles (1983) use the same approach as Charles-Edwards and Thornley (1973), but also treat radiation scattered by the canopy, and provide for foliage density to be a function of position in the canopy. None of these three models is presented in terms of calculating the apparent canopy reflectance as a function of view angle, however.

Soil reflectance models have not been so prevalent. Kimes (1983) presents some bidirectional reflectance data of bare soil, and discusses some of the factors that influence the shape of the distribution. Walthall et al. (1985) use a simple empirical equation to fit some observations of bidirectional reflectance factors of three soil surfaces differing in roughness. Cooper and Smith (1985) present a three dimensional Monte Carlo model for soil reflectance. The model considers surface irregularities larger than the wavelength of incident flux, but is never compared with field measurements. A simple model, which considers only geometric shading from a rectangular block, is presented in Norman et al. (1985). Although the model can be made to fit observations quite well, the number of required parameters is inconveniently large. A two-parameter shading model based on spherical soil particles (Campbell et al.) is presented in Appendix C.

The model presented in this paper is based upon the one of Norman and Welles (1983). The general model is reviewed briefly, and the formulations for predicting bidirectional reflectance are given. The

spherical model of Campbell et al. (Appendix C) is used as a boundary condition for soil BRDF. Finally, the model is compared to field measurements in a soybean canopy at three different stages of growth, and a corn canopy at 2 stages of growth.

THEORY

Norman and Welles (1983) describe a 3 dimensional radiative transfer model for vegetation (GAR, for General Array Model). The GAR model makes the following assumptions: 1) The entire plant canopy is made up of subcanopies whose outer envelope is defined by a regular array of ellipsoids. Subcanopies are usually individual plants or, where appropriate, entire rows. 2) Ellipsoids are optionally chopped horizontally at the top and/or bottom. 3) Foliage within an ellipsoidal envelope can have any arbitrary distribution of zenith angle, but random azimuth angle. 4) Foliage within an ellipsoidal envelope is either uniformly ditributed, else sub-shells can be specified within which the foliage has different densities and angle distributions. These subshells are also ellipsoidal, and entirely contained - but not necessarily concentric - within the main outer ellipsoid. A decidous tree with most of its leaves located near the outside of the crown is an example of the type of canopy that lends itself well to this method of specifying ellipsoidal shells of constant foliage attributes. 5) A degree of randomness may be assigned to the subcanopies being located exactly where they are supposed to be in a regular array (e.g. within-row randomness). Also, there can be a finite chance of any particular ellipsoid being missing. 6) Direct beam interception is calculated for a particular location based upon the path length through subcanopies and the foliage properties contained therein. 7) Diffuse interception for a location is calculated by integrating the direct beam interception relation over the appropriate hemisphere. 8) Scattered radiation for a particular location is calculated by solving multiple scattering layer equations for a uniform canopy. This uniform canopy is generated such that one of the layers has the same diffuse transmittance up and down that the 3 dimensional canopy grid location has.

The bidirectional reflectance model (BIGAR3) described herein differs from GAR in two major areas: 1) The method of specifying the pattern or distribution of the subcanopies is more general and flexible. 2) the addition of the bidirectional computations.

BIGAR3 allows any distribution of subcanopies without having to specify the location and size of every one in the total canopy. The method used is to define all of the crowns within an arbitrary box, and then replicate the box as often as in necessary to simulate the horizontal extent of the canopy. If a subcanopy extends beyond the box, it is ignored. A row crop can be simulated (Fig 1a) by specifying the box to be a short segment of the row, and putting one subcanopy inside of the box. The subcanopy radius in the row direction is large compared to the box to keep the cross section uniform. By replicating this box many times in all directions, a field of rows is produced. An orchard can be simulated by putting one crown in a box, or, if the arrangement is staggered as in Fig 1b, one subcanopy can be put in the center of the box, and a quarter canopy in each corner. A deciduous forest can be simulated (Fig 1c) by putting enough subcanopies into the box to generate the randomness needed, then replicating the box many times in all directions.

GAR allows the calculation of the components of the radiative environment at any point in a canopy. These components are the direct beam radiation from the sun, the diffuse radiation from the sky and soil, and the diffuse radiation scattered by other foliage. BIGAR3 builds upon these formulations to predict the brightness of the scene as viewed from any direction. This is done by calculating the amount of radiation scattered toward the viewer from "all" points in the scene, weighting each by how well the viewer can see that particular point. In practice, a set of grid points is used, equally spaced in the vertical and horizontal throughout the box. If a grid point is outside of a subcanopy, it is ignored. Grid points within subcanopies are assumed to have a certain amount of foliage associated with it, determined by the grid spacing. The spacing of grid points within a box is somewhat arbitrary; they should be of sufficient density to represent the smallest subcanopies without making the computational time prohibitively expensive. There is a minimum grid spacing criteria that arises from an assumption used to calculate the

fraction of sunlit leaves for a grid point. It is important note that the canopy is described analytically by the ellipsoidal subcanopies; it is not digitized into the grid points. Thus, for example, if a particular subcanopy failed to encompass a grid point, that subcanopy would still contribute to the radiant flux calculations done at all grid points; it would not, however, directly contribute to the summed radiance computed in any direction.

The radiance of a canopy $[R_c(\theta_v,\phi_v)]$ as viewed from some direction (θ_v,ϕ_v) is assumed to depend upon two things: the radiance of the foliage elements, and how well they are seen. Thus,

$$R_c(\theta_v,\phi_v) = \sum_{i=1}^{N} W'_i \int_\alpha \int_\beta g(\alpha,\beta)\ R_i(\alpha,\beta)\ f'_v\ d\beta\ d\alpha \tag{1}$$

W'_i is a factor (normalized to sum to unity) that weights each grid point by how well it is seen by the viewer.

$$W'_i = \frac{\exp(-k\ \mu\ S_{vi})}{\sum_{j=1}^{N} \exp(-k\ \mu\ S_{vj})} \tag{2}$$

where S_{vi} is the distance through foliage between the ith grid point and the edge of the canopy in the direction of the viewer. f'_v is also a weighting factor (normalized to integrate to unity for all leaf angle classes) that essentially is the cosine of the angle between the leaf normal and the viewer. Thus, for example, a leaf whose edge is perfectly aligned with the viewer will contribute nothing to the radiance, whereas a leaf whose normal is pointed toward the viewer will contribute maximally.

$$f'_v = \frac{|f_v|}{\int_\alpha \int_\beta |f_v|\ d\beta\ d\alpha} \tag{3}$$

where

$$f_v = \cos\theta_v \cos\alpha + \sin\theta_v \sin\alpha \cos(\phi_v - \beta)$$

The radiance $[R_i(\alpha,\beta)]$ from foliage at angle (α,β) at the ith grid point is a combination of scattered diffuse irradiance, and scattered direct solar irradiance.

$$R_i(\alpha,\beta) = R_{bi}(\alpha,\beta)\ C_i + R_{di}(\alpha) \tag{4}$$

C_i is the fraction of sunlit leaves at the ith grid point, and $[R_{bi}(\alpha,\beta)]$ is the radiance from sunlit leaves of angle class (α,β). To calculate C_i, consider first an imaginary layer of foliage centered on the ith grid point. Assume that the foliage about this grid point is uniform having an extinction coefficient of k, and the solar zenith angle is θ.

The fraction C of leaves in this imaginary layer that are sunlit can be expressed as the sunlit leaf area index of that layer divided by the total leaf area index of that layer:

$$C = \frac{F_{sunlit}}{F_{total}}$$

$$C = \frac{\int_{F_1}^{F_2} \exp(-k\ \mu\ F/\cos\theta)\ dF}{F_2 - F_1}$$

$$C = \frac{\exp(-k\ \mu\ F_1/\cos\theta) - \exp(-k\ \mu\ F_2/\cos\theta)}{k\ \mu\ F_2/\cos\theta \quad k\ \mu\ F_1/\cos\theta} \tag{5}$$

The problem with this formulation for a uniform layer is how to define the "top" and "bottom" of a grid point. The question can be avoided by an approximation: If we note that

$$\frac{\exp(-a) - \exp(-b)}{b - a} \simeq \exp(-(a+b)/2) \quad \text{for } |b - a| < 0.5 \tag{6}$$

we can express the fraction of sunlit leaves as the beam transmittance to the layer midpoint in a uniform canopy, or the transmittance to a point in a non-random canopy. Thus, the fraction of sunlit leaves at the ith grid location is

$$C_i \simeq \exp(-k\,\mu\,S_{si}) \tag{7}$$

This approximation introduces a criteria for the grid spacing. For the 1% approximation, we need $(k\mu\Delta S)<0.5$, where ΔS is the grid spacing. If we take k to be on the average 0.5, then

$$\Delta S < \frac{1}{\mu} \tag{8}$$

This is usually not the only criteria for grid spacing; the grid should in general be fine enough to include representative points within the smallest sub-canopies of the canopy.

Radiance $[R_{bi}(\alpha,\beta)]$ from sunlit leaves of angle class (α,β) is the product of the incident irradiance and the reflectance or transmittance, depending upon whether or not the viewer and the sun see the same side of the leaf:

$$R_{bi}(\alpha,\beta) = \frac{E_t\ f_b\ |f_s|}{\cos\theta_s}\ \sigma_b \tag{9}$$

where E_t is the total irradiance on the horizontal above the canopy, f_b is the fraction of the total that is direct beam radiation, and f_s is the cosine of the angle between the sun and the leaf normal.

$$f_s = \cos\theta_s\ \cos\alpha + \sin\theta_s\ \sin\alpha\ \cos(\phi_s - \beta) \tag{10}$$

Note that

$$\sigma_b = \begin{cases} \rho & \text{if } f_s \text{ and } f_v \text{ are of the same sign} \\ \tau & \text{if } f_s \text{ and } f_v \text{ are of different signs} \end{cases} \quad (11)$$

Radiance [$R_{di}(\alpha)$] from leaves of inclination angle class (α) that is due to diffuse irradiance has four components. If the leaf is not level ($\alpha \neq 0$), the upper surface will see downward diffuse irradiance (D_i) and upward diffuse irradiance (U_i) in proportions of $(1+\cos\alpha)/2$ and $(1-\cos\alpha)/2$ respectively. Similarly, the lower surface will scatter both upward and downward diffuse irradiance, thus

$$R_{di} = \frac{(1+\cos\alpha)(D_i\ \sigma_d + U_i\ \sigma_u) + (1-\cos\alpha)\ (D_i\ \sigma_u + U_i\ \sigma_d)}{2} \quad (12)$$

where

$$\sigma_d = \begin{cases} \rho & \text{if } f_v>0 \\ \tau & \text{if } f_v<0 \end{cases} \qquad \sigma_u = \begin{cases} \tau & \text{if } f_v>0 \\ \rho & \text{if } f_v<0 \end{cases}$$

The diffuse fluxes D_i and U_i are calculated for the ith grid location by the method used in GAR, in which the diffuse transmittance for the upper and lower hemispheres for that grid point are used to to create a uniform, homogeneous canopy having some layer with matching diffuse transmittances. The diffuse fluxes are then calculated for this layer using the equations presented by Norman and Jarvis (1975). One of the boundary conditions used is that the beam transmittance for this particular layer matches the beam transmittance of the ith grid point.

A bidirectional reflectance distribution function (BRDF) is generated from BIGAR3 by selecting the spectral properties that are appropriate for the desired spectral wavelength band, and computing Eq. (1) for a set of view directions (θ_v,ϕ_v).

METHOD AND MATERIALS

BIGAR3 is tested by simulating BRDFs measured on corn and soybeans through the summer of 1982 using an Exotech multiband radiometer (Ranson et al. 1984, 1985). Although 4 spectral bands were measured, only the first (VIS: .5μm - .6μm) and the fourth (NIR: .8μm - 1.1μm) are simulated. Three dates are chosen for each crop through the growing season, and highest and lowest sun angles for each date. Tables 1 and 2 summarize the conditions for the tests.

The dimensions of the simulated canopy are determined by direct measurements of the height and row spacing, and percent cover. Measurements of LAI (F) are converted to foliage density (μ) by the following equation:

$$\mu = \frac{F\ A_g}{V_c} \quad (13)$$

where A_g is ground area, and V_c is volume of canopy. Since the both canopies were planted in rows, the box dimensions are taken to be 1 m along the row, width equal to the row spacing, and height equal to the canopy height. One subcanopy is placed inside this box at the center. The vertical radius is one-half the box height, the in-row radius is 100m so that the 1m of canopy within the box is essentially of uniform cross section, and the cross-row radius based on estimates of canopy cover. With this arrangement, Eq. (13) can be re-written as

$$\mu = \frac{F\ B_X\ B_y}{B_y\ \pi\ R_X\ R_Z} \tag{14}$$

where B_X and B_y are the box cross-row and in-row dimensions, and R_X and R_Z are the subcanopy cross-row and vertical radii.

Two azimuthal transformations must be done on the results of BIGAR3 in order to compare them to the measured BRDF's. For a given azimuth angle of view, BIGAR3 calculates a radiance leaving the canopy, whereas the direct measurements report azimuth looking toward the canopy. Thus, BIGAR3 results must be rotated 180°. In addition, BIGAR3 uses a mathematical coordinate system, whereby azimuth angles are measured counterclockwise from the +X axis. The +X axis is usually assumed to be pointing east, but this is arbitrary. The measured BRDFs are reported using azimuth angles measured clockwise from north.

RESULTS

Figures 2 and 3 illustrate measured (DATA) and predicted (MODEL) BRDFs for corn and soybeans, each at three different dates, and two sun angles and two wavebands per date using a 3 dimensional perspective of the BRDF in polar coordinates. The distance from the center of a BRDF surface corresponds to view zenith angle (θ_V); the maximum zenith angle is 70° for the corn data, and 60° for the soybeans. Moving around the figure corresponds to changing view azimuth angle (ϕ_V). The view azimuths are labelled on the front two sides of each figure. These azimuth angles are measured clockwise relative to north. The height of the figures is corresponds to a reflectance in percent, and the vertical scale is indicated on each figure. The measured BRDFs in some cases contained regions of missing data. In preparing the plots, missing data are assigned a value of 0, so such regions appear as holes or eroded edges in the figures.

DISCUSSION

In general, the BIGAR3 does fairly well in predicting the character of the BRDF surface. The brightest areas tend to be at the antisolar point, although the presence of corn plants tend to smooth out the distinctiveness of it to the point where the surface has a tilted bowl appearance at an LAI of 4.4 (Fig. 2e and 2f). The soybeans exhibit a distinct hotspot (Fig 3a and 3c) in the visible that is only hinted at by the model. In fact, with the exception of the June 25 corn data (Fig 2c and 2d), the model tends to underestimate the extremes of the BRDF besides the hot spot.

The June 13 corn BRDFs (Fig 2a and 2b) show an interesting transition region between high and low view zenith angles. Both the measurements and the model show the relative brightness of the soil at the antisolar point, a fairly rapid decrease as view angles move away from this point, and then a plateau or even an increase again at oblique angles where the sparse plants effectively hide the soil.

The row structure of both crops is evident in general as a N-S trough that runs through the BRDF surface. Not surprisingly, the trough tends to be more evident in the NIR where the contrast between soil reflectance and leaf reflectance is greater. In corn, the trough is most evident in both the model and the measurements in the June 25 data, when the rows are fairly dense but still well separated.

The June 13 corn case was also simulated by specifying the canopy on a plant-by-plant basis, rather than row-by-row. The results were quite comparable, although the computation time was much increased.

LIST OF SYMBOLS

C_i	Fraction of leaves that are sunlit at ith grid point.
D_i	Downward diffuse irradiance from the upper hemisphere at the ith point.
E_t	Total incident irradiance on the horizontal at the top of the canopy.
N	Number of grid points that lie in subcanopy.
R_{bi}	Radiance from foliage at ith point due to direct beam irradiance.
R_c	Radiance from the canopy in direction (θ_V,ϕ_V).
R_{di}	Radiance from foliage at ith point due to diffuse irradiance.
R_i	Total radiance from foliage at ith point.
S_{si}	Distance from ith grid to canopy edge toward sun.
S_{vi}	Distance from ith grid to canopy edge toward viewer.
U_i	Upward diffuse irradiance from the lower hemisphere at the ith point.
W'_i	Weighting factor of ith point for the viewer, normalized to unity.
α	Leaf tilt angle.
β	Leaf azimuth angle.
f_s	Cosine of the angle between the leaf normal and the sun.
f_v	Cosine of the angle between the leaf normal and the viewer.
f_b	Fraction of the total incident irradiance that is direct beam.
$g(\alpha,\beta)$	Fraction of leaf area at leaf angle class (α, β).
k	Canopy extinction coefficient.
μ	Foliage area density (leaf area per canopy volume).
ϕ_s	Solar azimuth angle.
ϕ_V	View azimuth angle.
ρ	Leaf reflectance.
σ_b	Leaf transmittance or reflectance, depending on view and sun angles.
σ_d	Leaf transmittance or reflectance, depending on view angle.
σ_u	Leaf transmittance or reflectance, depending on view angle.
τ	Leaf transmittance.
θ_s	Solar zenith angle.
θ_V	View zenith angle.

LITERATURE CITED

Allen Jr., L. H. (1974). Model of light penetration into a wide-row crop. *Agron. J.* 66:41-47.

Arkin, G. F., J. T. Richie, and S. J. Maas (1978). A model for calculating light interception by a grain sorghum canopy. *Trans. ASAE.* 21:303-308.

Campbell, G. S., J. M. Norman, and J. M. Welles (Appendix C). Test of a simple model for predicting bidirectional reflectance of a bare soil surface.

Charles-Edwards, D. A. and J. H. M. Thornley (1973). Light interception by an isolated plant: A simple model. *Ann. Bot.*37:919-928.

Charles-Edwards, D. A. and M. R. Thorpe (1976). Interception of diffuse and direct-beam radiation by a hedgerow apple orchard. *Ann. Bot.* 40:603-613.

Cooper, K. D. and J. A. Smith (1985). A Monte Carlo reflectance model for soil surfaces with three-dimensional structure. *IEEE Trans. Geosci. and Remote Sens.* GE-23:668-673.

Gerstl, S. A. W. and A. Zardecki (1985). Discrete-ordinates finite-element method for atmospheric radiative transfer and remote sensing. *Appl. Optics* 24:81-93.

Goel, N. S. and T. Grier (1986a). Estimation of canopy parameters for inhomogeneous vegetation canopies from reflectance data. *Int. J. Remote Sens.* 7:665-681.

Goel, N. S. and T. Grier (1986b). Estimation of canopy parameters of row planted vegetation canopies using reflectance data for only 4 view directions. *Remote Sens. Environ.*

Kimes, D. S. (1983). Dynamics of directional reflectance factor distributions for vegetation canopies. *Appl. Optics* 22:1364-1372.

Kubelka, P. and F. Munk (1931). Ein beitrag zur optik der farbanstriche. *Ann. Techn. Phys.* 11:593-601.

Mann, J. E., G. L. Curry and P. J. H. Sharpe (1979). Light interception by isolated plants. *Agric. Meteorol.* 20:205-214.

Mann, J. E., G. L. Curry, D. W. DeMichele, and D. N. Baker (1980). Light penetration in a row crop with random plant spacing. *Agron. J.* 72:131-142.

Nicodemus, F. E., J. C. Richmond, J. J. Hsia, I. W. Ginsberg, and T. Limperis (1977). Geometric considerations for nomenclature of reflectance. National Bureau of Standards Monograph 160. 52 pp.

Norman, J. M. and P. G. Jarvis (1975). Photosynthesis in Sitka Spruce (*Picae sitchensis* (Bong.) Carr.) V: Radiation penetration theory and a test case. *J. Appl. Ecol.* 12:839-878.

Norman, J. M. and J. M. Welles (1983). Radiative transfer in an array of canopies. *Agron J* 75:481-488.

Norman, J. M., J. M. Welles, and E. A. Walter (1985). Contrasts among bidirectional reflectance of leaves, canopies, and soils. *IEEE Trans. Geosci. and Remote Sens.* GE-23:659-667.

Palmer, J. W. (1977). Diurnal light interception and a computer model of light interception by hedgerow apple orchards. *J. Appl. Ecol.* 14:601-614.

Ranson, K. J., L. L. Biehl, and C. S. T. Daughtry (1984). Soybean canopy reflectance modeling data sets. LARS Tech. Report No. 071584. pp 46.

Ranson, K. J., C. S. T. Daughtry, L. L. Biehl, and M. E. Bauer (1985). Sun-view angle effects on reflectance factors of corn canopies. *Remote Sens. Environ.* 18:147-161.

Suits, G. H. (1972). The calculation of the directional reflectance of a vegetative canopy. *Remote Sens. Environ.* 2:117-125.

Suits, G. H. (1983). The extention of the uniform canopy reflectance model to include row effects*Remote Sens. Environ.* 13:113-129.

Verhoef, W. (1984). Light scattering by leaf layers with application to canopy reflectance modeling: The SAIL model. *Remote Sens. Environ.* 16:125-141.

Verhoef, W. and N. J. J. Bunnik (1975). A model study on the relations between crop characteristics and canopy spectral reflectance *NIWARS* Publ. No. 33, 3 Kanaalweg, Delft, The Netherlands.

Walthall, C. L., J. M. Norman, J. M. Welles, G. S. Campbell, and B. L. Blad (1985). A simple equation to approximate the bidirectional reflectance from vegetative canopies and bare soil surfaces. *Appl. Optics* 24:383-387.

Whitfield, D. M. (1986). A simple model of light penetration into row crops. *Agric. and For. Meteorol.* 36:297-315.

Table 1

	CORN			SOYBEANS		
	6/13	6/25	8/12	7/17	7/24	8/27
Soil Reflectance VIS	.08	.08	.08	.09	.09	.09
Soil Reflectance NIR	.18	.18	.18	.19	.19	.19
Soil SAI	.5	.5	.5	.5	.5	.5
Leaf reflectance VIS	.07	.07	.07	.09	.09	.09
Leaf reflectance NIR	.38	.38	.38	.45	.45	.45
Leaf transmittance VIS	.03	.03	.03	.09	.09	.09
Leaf transmittance NIR	.55	.55	.55	.52	.52	.52
Foliage density	5.38	6.9	2.12	7.25	7.48	4.4
Box width	.76	.76	.76	.76	.76	.76
Box height	.4	.56	2.8	.69	.84	.84
Box length	1.0	1.0	1.0	1.0	1.0	1.0
Subcanopy height radius	.2	.28	1.4	.35	.42	.42
Subcanopy width radius	.09	.15	.36	.29	.30	.38
Subcanopy length radius	100	100	100	100	100	100
Grid points (widthxheight)	15x8	15x11	5x18	10x9	8x10	8x10
Grid points (widthxheight)	15x8	15x11	5x18	10x9	8x10	8x10

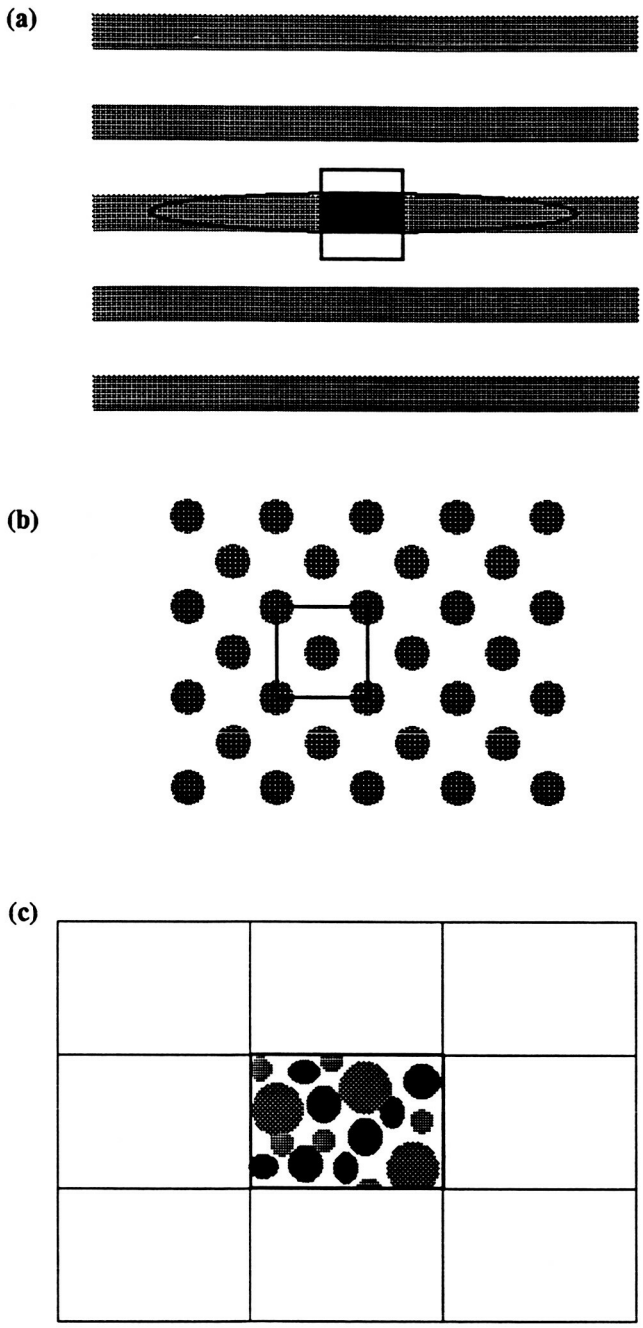

Figure 1. Representations of three types of canopies with the BIGAR3 model. **a).** Row crop. **b).** Orchard. **c).** Mixed hardwood forest. See text for discussion.

Figure 2. Comparison of modeled and measured canopy bidirectional reflectance factors for corn for two solar zenith angles, two wavelength bands, and three dates: June 13, 1982 (a and b); June 25, 1982 (c and d); and August 12, 1982 (e and f).

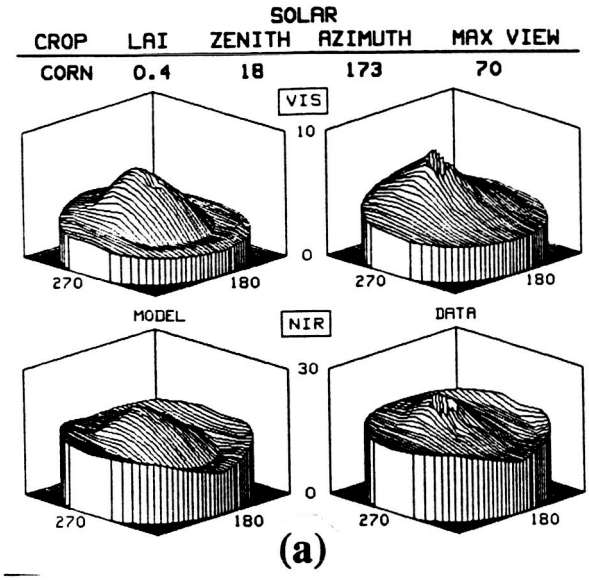
SOLAR
CROP LAI ZENITH AZIMUTH MAX VIEW
CORN 0.4 18 173 70
VIS
10
0
270
180
MODEL
NIR
DATA
30
0
270
180

(a)

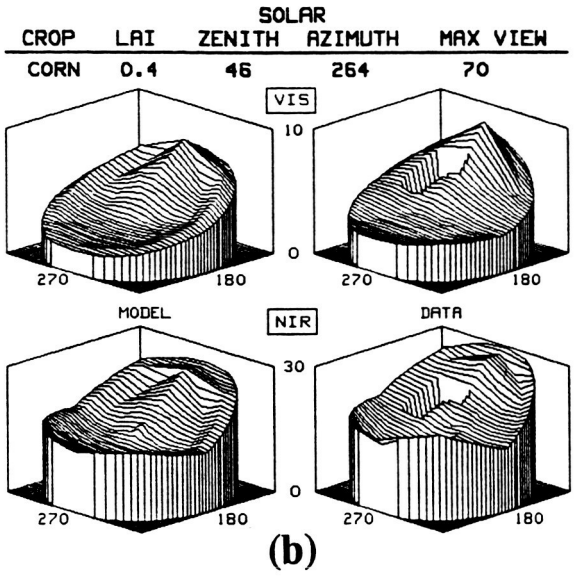
SOLAR
CROP LAI ZENITH AZIMUTH MAX VIEW
CORN 0.4 46 264 70
VIS
10
0
270
180
MODEL
NIR
DATA
30
0
270
180

(b)

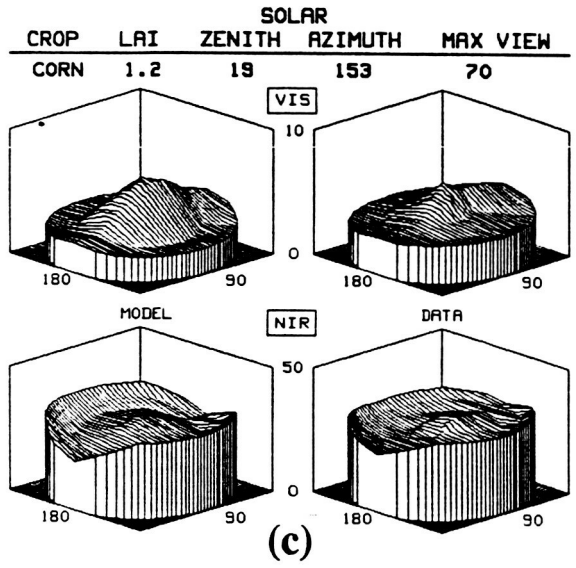
SOLAR
CROP LAI ZENITH AZIMUTH MAX VIEW
CORN 1.2 19 153 70
VIS
10
0
180
90
MODEL
NIR
DATA
50
0
180
90

(c)

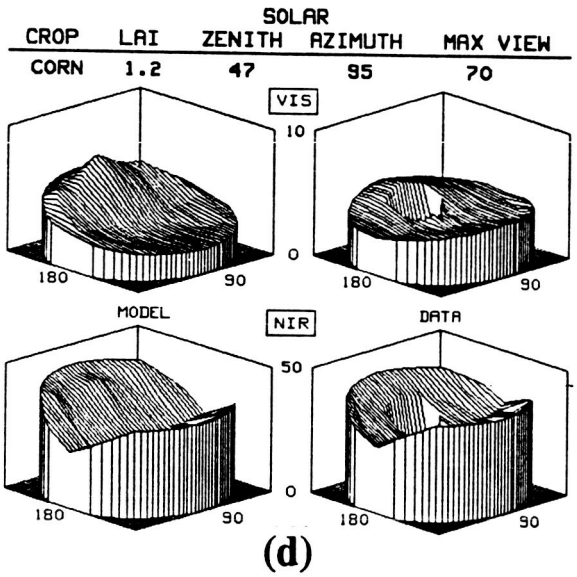
SOLAR
CROP LAI ZENITH AZIMUTH MAX VIEW
CORN 1.2 47 95 70
VIS
10
0
180
90
MODEL
NIR
DATA
50
0
180
90

(d)

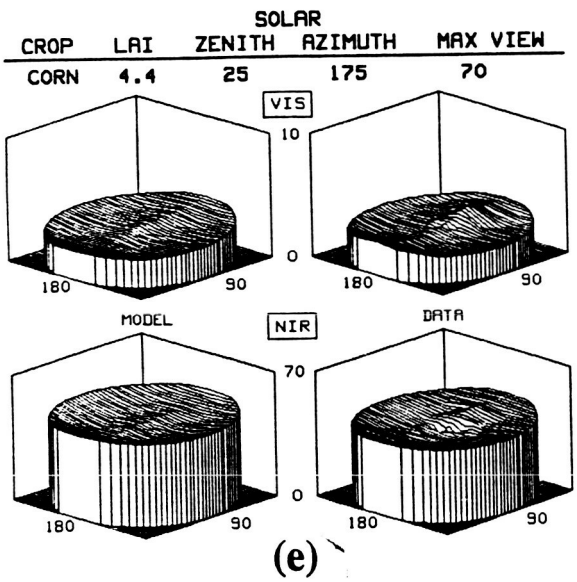
SOLAR
CROP LAI ZENITH AZIMUTH MAX VIEW
CORN 4.4 25 175 70
VIS
10
0
180
90
MODEL
NIR
DATA
70
0
180
90

(e)

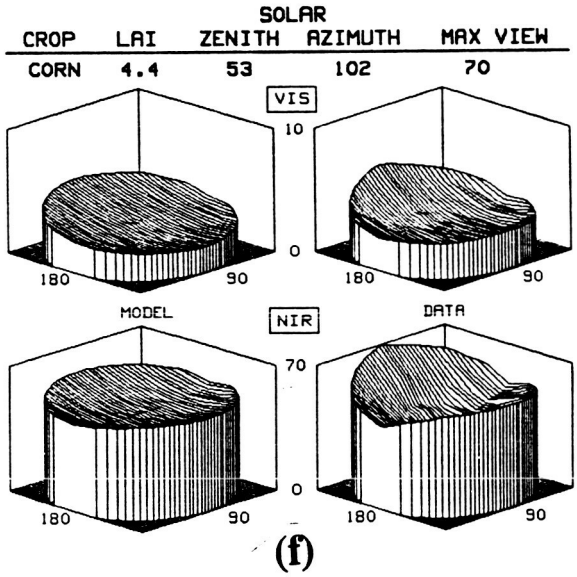
SOLAR
CROP LAI ZENITH AZIMUTH MAX VIEW
CORN 4.4 53 102 70
VIS
10
0
180
90
MODEL
NIR
DATA
70
0
180
90

(f)

Figure 3. Comparison of modeled and measured canopy bidirectional reflectance factors for soybeans for two solar zenith angles, two wavelength bands, and three dates: July 17, 1982 (a and b); July 24, 1982 (c and d); and August 27, 1982 (e and f).

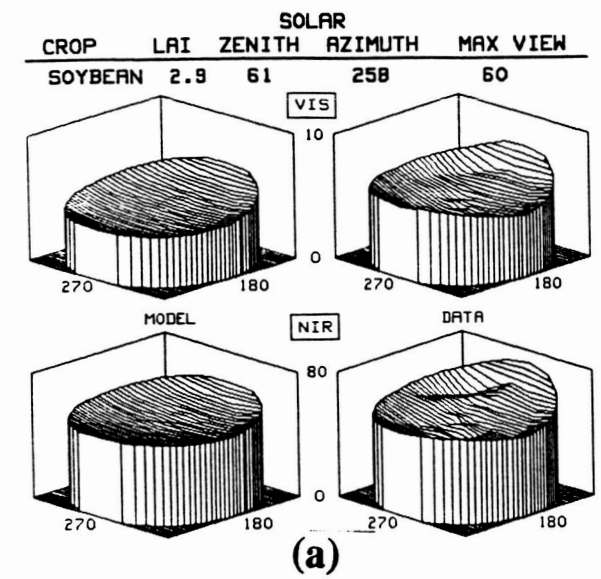
SOLAR
CROP LAI ZENITH AZIMUTH MAX VIEW
SOYBEAN 2.9 61 258 60
VIS
10
0
270
180
MODEL
NIR
DATA
80
(a)

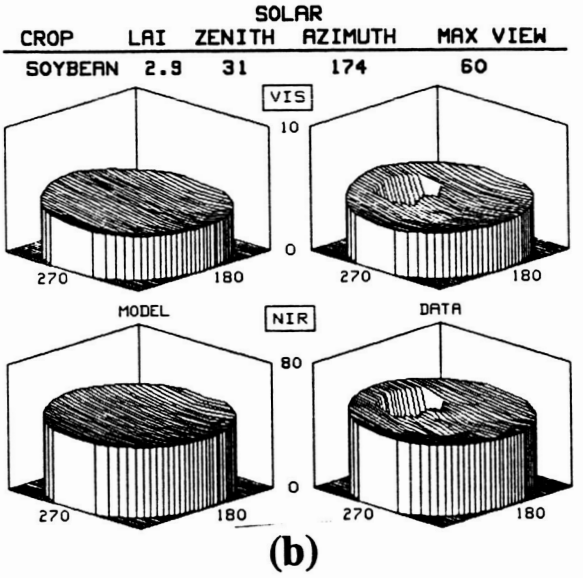
SOLAR
CROP LAI ZENITH AZIMUTH MAX VIEW
SOYBEAN 2.9 31 174 60
VIS
10
0
270
180
MODEL
NIR
DATA
80
(b)

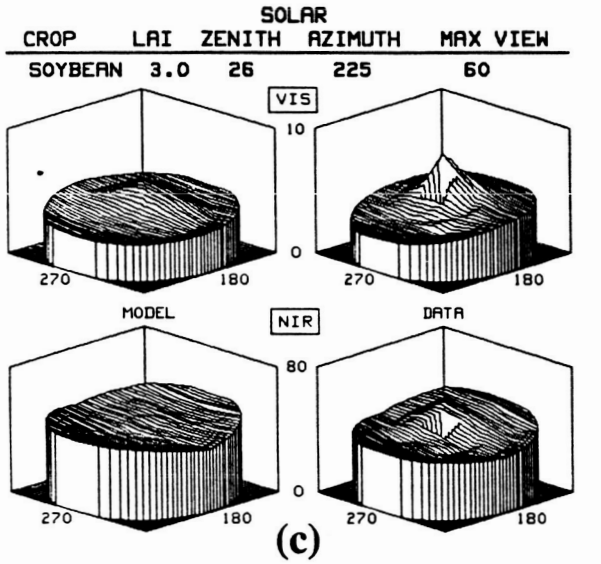
SOLAR
CROP LAI ZENITH AZIMUTH MAX VIEW
SOYBEAN 3.0 26 225 60
VIS
10
0
270
180
MODEL
NIR
DATA
80
(c)

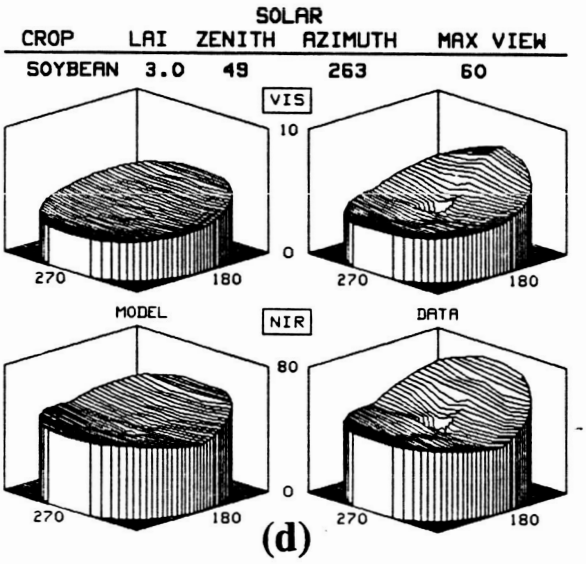
SOLAR
CROP LAI ZENITH AZIMUTH MAX VIEW
SOYBEAN 3.0 49 263 60
VIS
10
0
270
180
MODEL
NIR
DATA
80
(d)

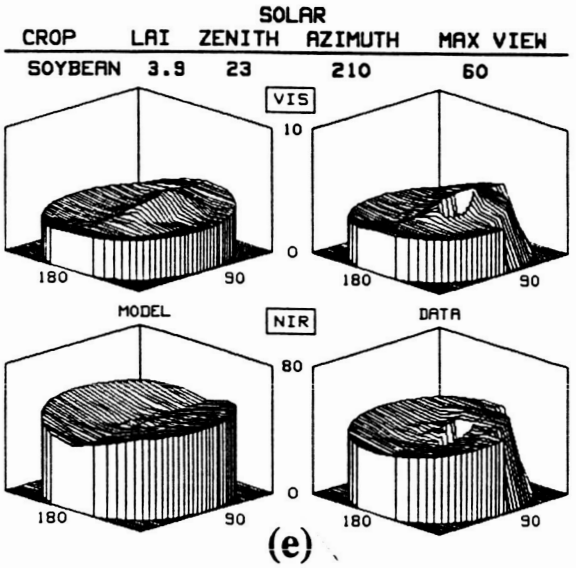
SOLAR
CROP LAI ZENITH AZIMUTH MAX VIEW
SOYBEAN 3.9 23 210 60
VIS
10
0
180
90
MODEL
NIR
DATA
80
(e)

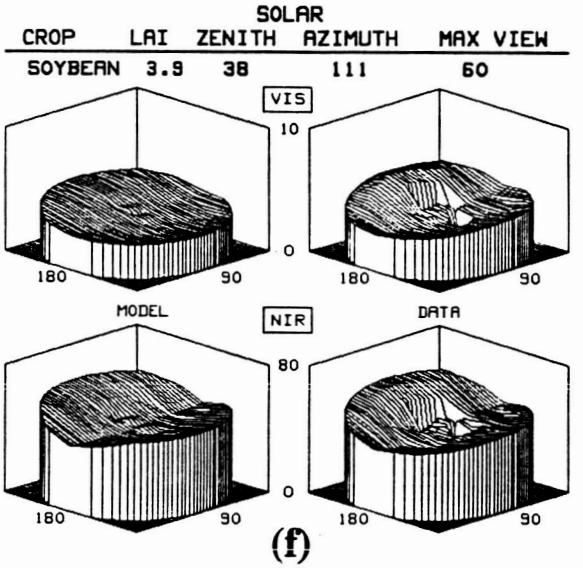
SOLAR
CROP LAI ZENITH AZIMUTH MAX VIEW
SOYBEAN 3.9 38 111 60
VIS
10
0
180
90
MODEL
NIR
DATA
80
(f)

APPENDIX C

Preliminary draft of a paper on modeling soil bidirectional reflectance that provides development of a sphere model and comparisons with measurements.

Campbell, G. S., J. M. Norman and J. M. Welles. 1988. Test of a simple model for predicting bidirectional reflectance of a bare soil surface.

TEST OF A SIMPLE MODEL FOR PREDICTING BIDIRECTIONAL REFLECTANCE OF A BARE SOIL SURFACE

G. S. Campbell and J. M. Norman

Abstract

The bidirectional reflectance of a soil surface was simulated by uniform spheres on a flat surface. Three parameters were used to describe the bidirectional reflectance pattern: the sphere area index (vertically projected area of spheres per unit area of flat surface, the fraction of incident radiation which is diffuse, and the reflectance of the soil material. Predictions from the model agree well with measured bidirectional reflectance patterns of soil surfaces. Comparisons with empirical equations are also presented.

Introduction

The bidirectional reflectance pattern of a soil surface can be used in at least two ways. It can give information about the characteristics of the soil surface, and can also be used as the lower boundary condition for crop canopy reflectance models. As canopies become sparse, the bidirectional pattern of the soil surface has an increasing effect on the overall pattern observed above the crop.

Although bidirectional patterns of canopies have been studied in some detail, (cf. Smith and Ranson, 1979; Suits, 1972; Chen, 1984), patterns for soil surfaces have received far less attention. An empirical equation with a fit to some data was presented by Walthall et al. (1985), and a simple model which simulated the soil surface as a flat surface covered with iniform blocks of a specified length, width, and height, was presented by

Norman et al. (1985). While both of these models fit available data reasonably well, they are not as useful as they could be. The empirical equation does not take into account changes in the fraction of diffuse radiation and the coefficients are not easily related to the properties of the soil surface. The dimensions used in the block model are rather arbitrary, and it works satisfactorily for only a limited range of beam elevation angles. It therefore seemed desirable to develop a model in which the properties of the soil surface were more clearly related to the model parameters. This would not only allow reliable prediction of soil bidirectional reflectance, but would simplify the inversion of soil BDR patterns to get soil surface properties.

A model which is simple, yet close to reality is that of uniform spheres on a flat surface. The shadow areas of spheres, as well as their BDR patterns are easily calculated (Egbert, 1977). Predictions of such a model will be compared to measured BDR patterns for a range of soil roughness. Predictions from this model will also be compared to those from the empirical equations from Walthall et al. (1985).

Model

The model used here is similar to that of Egbert (1977), except that reflectance is assumed to be entirely Lambertian. The soil surface is assumed to be simulated by uniform spheres, regularly spaced on a flat surface. The spheres and the surface are assumed to have a reflectance of ρ. A sphere area index, L, is defined as the area of vertical projections of spheres per unit area of plane surface. The scene is assumed lit by both beam and diffuse radiation, with the fraction of total radiation on a horizontal surface which is diffuse being represented by f. The beam radiation on a horizontal surface is therefore 1-f.

The relative areas of sphere, shadow, and sunlit plane which are seen

from a given look angle can be determined by considering a single sphere in a circle of unit area. The fractional area of shadow cast on the plane by the sphere, when the solar elevation angle is ϕ_b is

$$A_s = L/\sin \phi_b \quad . \tag{1}$$

The fractional area of sphere, A_v, viewed from an elevation angle, ϕ_v is given by eq. 1, with ϕ_b replaced by ϕ_v. The fractional area of shadow which cannot be seen from a given view angle depends on the view azimuth, ψ, as well as on the view and beam elevations. The overlap area was found by numerical integration, and then fit by the empirical function

$$A_{ovl} = A_s \exp(-A\theta^2 - B\theta) \tag{2}$$

where θ is the minimum angle between the beam and view directions, given by

$$\cos\theta = \sin \phi_b \sin\phi_v + \cos \phi_b \cos \phi_v \cos \psi \quad . \tag{3}$$

The coefficients A and B depend on beam angle, and are given by

$$A = 1.165 \phi_b^3 - 4.108 \phi_b^2 + 4.824 \phi_b - 1.652$$

$$B = -2.666 \phi_b^3 + 9.588 \phi_b^2 - 11.749 \phi_b + 5.51 \quad .$$

The rms errors in the values from eq. 2 are less than 3% for beam and view elevation angles ranging from 15 to 75 degrees.

The fractional area of the plane which is sunlit and seen from a given view angle is

$$A_{sl} = 1 - A_s - A_v + A_{ovl} \tag{4}$$

with the additional condition that A_{sl} must not be negative. A_v is also constrained so that it does not become greater than unity at low sun angles. At low angles, shadows start to overlap.

The bidirectional reflectance of the surface can now be calculated from

$$R = \rho f + \rho(1-f)\{A_{sl} + A_v[\sin \theta + (\pi-\theta)\cos \theta]/2\sin \phi_b\}. \tag{5}$$

The final term represents the reflectance of a sphere. The average irradiance of a hemisphere is half that of a plane perpendicular to the solar beam. The intensity of reflected beam radiation is therefore half

that for a plane perpendicular to the beam when the view and beam angles are the same, and decreases as the angle between beam and view directions increases.

Experimental

Measurements of bidirectional reflectance were made for several surfaces ranging in roughness from gravel-covered parking lots to recently-plowed sod fields. Fisheye pictures of the surfaces are shown in Fig. 1. along with short descriptions of each location.

Measurements were made using a silicon sensor which was mounted behind a 16 mm movie camera lens which had a focal length of . The lens was mounted on the shaft of a small, dc gear motor which was mounted on a frame so that the lens would rotate around an axis perpendicular to the soil surface at a height of about 1.5 m. The angle of the lens, relative to the axis of the motor was adjustable, so that various view angles could be set. The motor was driven by a data logger (Model CR21X, Campbell Scientific, Inc. , Logan Utah). A switch was set to close at the home location of the radiometer, which was always set to be directly opposite the azimuth angle of the sun. For each view elevation angle, the data logger would turn on the motor to start the radiometer rotating, and then sample about 200 times (depending on motor speed) while the radiometer rotated through 360 degrees.

Incoming and reflected global solar radiation were measured with Kipp solarimeters (Kipp and Zonen,). The solar elevation angle was measured with a protractor. The fraction of radiation which was diffuse was needed for the models, but was not measured. Estimates were therefore needed. These were calculated from measured global solar radiation values using equations from Campbell (1981) and then fit to a quadratic which gave the diffuse fraction for each beam elevation angle.

Two sets of measurements were taken. The first were made on

1983, and consisted of 8 sets of measurements on three surfaces, a rough plowed field of sod, a field which had received several tillage operations and a smooth gravel parking lot. Measurements were made at six view elevation angles ranging from 15 to 90 degrees in 15 degree increments. The second set of measurements was made on July 13, 1984 on two surfaces, a gravel parking lot, and a tilled field. The 1984 locations were not the same as those used for the 1983 measurements, but were similar in roughness to the parking lot and medium-till fields used in 1983. Twenty-seven sets of measurements were taken throughout the day, with half the measurements being made through a filter which eliminated visible radiation. Since we had no independent calibration of the sensor with the filter, the NIR data served mainly as a duplicate set for the unfiltered data.

All of the raw data were averaged over 30 degree azimuth angle increments, and values between 360 and 180 degrees were averaged with those from 0 to 180, since all of the models are assumed to be symmetric with respect to the beam azimuth angle. These averaged data sets were then used for fitting and testing the bidirectional reflectance models. A non-linear least squares procedure similar to that described by Goel and Thompson (1984) was used to find the model parameters which best fit each data set.

Results and Discussion

The model parameters which best fit the data are shown in Tables 1 and 2 for the two data sets. The fits to the data are generally good, with rms errors being mainly due to actual point to point fluctuations in the data, rather than systematic over- or underestimation at particular locations in the scene. Part of the variation in the data is due to the shadows cast by the radiometer on the scene.

Table 1. Soil reflectances (ρ) and sphere area index (L) values which best fit data from set 1 for rough, medium, and smooth surfaces. Rms errors are also shown.

Surface	ϕ_b(deg)	ρ	L	rms error
ROUGH1	22.5	0.2509	0.3158	0.0242
ROUGH2	27.0	0.3010	0.3397	0.0215
ROUGH3	60.0	0.2261	0.3170	0.0258
ROUGH4	70.0	0.1979	0.3338	0.0232
MEDIUM1	47.0	0.2520	0.5012	0.0104
MEDIUM2	62.0	0.2639	0.7620	0.0079
SMOOTH1	46.0	0.1645	0.6356	0.0116
SMOOTH2	52.0	0.1691	0.6946	0.0109

Table 2. Reflectances (ρ), sphere area index (L), and errors for data from set 2. Values are those for best fit of the sphere model by non-linear least squares.

Surface and filter	ϕ_b(deg)	ρ	L	rms error
TILLED FIELD - NO FILTER	13.0	0.4090	0.1901	0.0369
TILLED FIELD - NO FILTER	22.0	0.4581	0.2877	0.0245
TILLED FIELD - NO FILTER	43.0	0.3112	0.1971	0.0450
TILLED FIELD - NO FILTER	65.0	0.2874	0.1787	0.0304
TILLED FIELD - NO FILTER	68.0	0.2708	0.1578	0.0343
TILLED FIELD - NO FILTER	48.0	0.2919	0.1856	0.0484
TILLED FIELD - NO FILTER	38.0	0.3350	0.2066	0.0543
TILLED FIELD - NIR ONLY	13.0	0.5072	0.1906	0.0461
TILLED FIELD - NIR ONLY	22.0	0.5288	0.2816	0.0290
TILLED FIELD - NIR ONLY	43.0	0.3403	0.1852	0.0511
TILLED FIELD - NIR ONLY	65.0	0.2951	0.1425	0.0344
TILLED FIELD - NIR ONLY	68.0	0.2936	0.1343	0.0367
TILLED FIELD - NIR ONLY	48.0	0.3145	0.1618	0.0494
TILLED FIELD - NIR ONLY	38.0	0.3688	0.1906	0.0561
GRAVEL SURFACE - NO FILTER	12.0	0.4600	0.1821	0.0513
GRAVEL SURFACE - NO FILTER	20.0	0.3763	0.1317	0.0488
GRAVEL SURFACE - NO FILTER	42.0	0.2652	0.0479	0.0352
GRAVEL SURFACE - NO FILTER	62.0	0.2408	0.0413	0.0323
GRAVEL SURFACE - NO FILTER	64.0	0.2104	-0.0324	0.0372
GRAVEL SURFACE - NO FILTER	38.0	0.2932	0.1057	0.0554
GRAVEL SURFACE - NIR ONLY	10.0	0.4372	0.1545	0.0327
GRAVEL SURFACE - NIR ONLY	20.0	0.3393	0.1149	0.0456
GRAVEL SURFACE - NIR ONLY	41.0	0.2190	0.0024	0.0297
GRAVEL SURFACE - NIR ONLY	62.0	0.2007	0.0163	0.0289
GRAVEL SURFACE - NIR ONLY	64.0	0.1884	-0.0348	0.0271
GRAVEL SURFACE - NIR ONLY	38.0	0.2532	0.0841	0.0541
GRAVEL SURFACE - NIR ONLY	29.0	0.2974	0.1356	0.0639

The parameters ρ and L are generally consistent for a particular surface, with variations possibly resulting from the fact that each set of measurements was made at a different location. There appears to be a systematic increase in reflectance at low solar elevation angles, which could be due to experimental errors, since measurements of global and reflected radiation is subject to large cosine errors at these low elevation angles, but could also possibly be from the failure of the model to properly account for possible specular backscattered radiation when the sun elevation angle is low and the view angle is close to the sun angle.

It was hoped that the sphere area index values would bear some relationship to the roughness of the soil surface, so that inversion of soil BDR measurements might be used to estimate soil roughness. The L values shown in Tables 1 and 2 do seem to indicate some property of the surface, but the relationship to surface roughness is unclear. The highest and lowest values are both for the gravel surfaces, which were the smoothest. The roughest surface was the next to lowest value. In addition, the gravel surface in Table 2 showed a variation of L with solar elevation angle, and even gave negative values (probably not significant) at midday.

The same non-linear least squares procedure used to fit the sphere model to the data was also used to fit the equation proposed by Walthall et al. (1985) to the data sets. The equation is

$$R = A\ \theta_v^2 + B\ \theta_v \cos\psi + C\ , \qquad (6)$$

where A, B, and C and coefficients to find, and θ_v is the view zenith angle. The coefficients and rms errors for this equation are shown in Tables 3 and 4 for the two data sets.

Table 3. Coefficients for eq. 6 fit to data from set 1 for rough, medium, and smooth surfaces. Rms errors are also shown.

Surface	ϕ_b(deg)	A	B	C	rms error
ROUGH1	22.5	0.0574	0.0851	0.0790	0.0281
ROUGH2	27.0	0.0441	0.0981	0.1103	0.0268
ROUGH3	60.0	-0.0201	0.0471	0.1516	0.0117
ROUGH4	70.0	-0.0221	0.0351	0.1384	0.0120
MEDIUM1	47.0	-0.0053	0.0538	0.1206	0.0145
MEDIUM2	62.0	-0.0198	0.0297	0.1384	0.0110
SMOOTH1	46.0	0.0086	0.0217	0.0720	0.0055
SMOOTH2	52.0	0.0015	0.0177	0.0791	0.0052

Table 4. Empirical coefficients and errors for non-linear least squares fits of eq. 6 to data from set 2.

Surface and filter	ϕ_b(deg)	A	B	C	rms error	
TILLED FIELD - NO FILTER	13.0	0.0882	0.1433	0.1513	0.0382	
TILLED FIELD - NO FILTER	22.0	0.0793	0.1363	0.1726	0.0348	
TILLED FIELD - NO FILTER	43.0	0.0076	0.0985	0.2140	0.0205	
TILLED FIELD - NO FILTER	65.0	-0.0370	0.0615	0.2468	0.0153	
TILLED FIELD - NO FILTER	68.0	-0.0278	0.0605	0.2365	0.0189	
TILLED FIELD - NO FILTER	48.0	0.0110	0.0964	0.2079	0.0199	
TILLED FIELD - NO FILTER	38.0	0.0320	0.1155	0.2045	0.0219	
TILLED FIELD - NIR ONLY	13.0	0.1196	0.1665	0.1822	0.0518	
TILLED FIELD - NIR ONLY	22.0	0.0907	0.1394	0.2041	0.0392	
TILLED FIELD - NIR ONLY	43.0	0.0118	0.1048	0.2380	0.0252	
TILLED FIELD - NIR ONLY	65.0	-0.0246	0.0613	0.2584	0.0195	
TILLED FIELD - NIR ONLY	68.0	-0.0214	0.0634	0.2594	0.0196	
TILLED FIELD - NIR ONLY	48.0	0.0135	0.0949	0.2336	0.0203	
TILLED FIELD - NIR ONLY	38.0	0.0323	0.1183	0.2364	0.0228	
GRAVEL SURFACE - NO FILTER	12.0	0.1425	0.0781	0.1578	0.0396	
GRAVEL SURFACE - NO FILTER	20.0	0.0828	0.0771	0.2155	0.0263	
GRAVEL SURFACE - NO FILTER	42.0	0.0393	0.0422	0.2219	0.0172	
GRAVEL SURFACE - NO FILTER	62.0	0.0139	0.0437	0.2198	0.0190	
GRAVEL SURFACE - NO FILTER	64.0	0.0336	0.0385	0.1984	0.0242	
GRAVEL SURFACE - NO FILTER	38.0	0.0614	0.0789	0.2063	0.0203	
GRAVEL SURFACE - NIR ONLY	10.0	0.1104	0.0837	0.1682	0.0320	0.3269
GRAVEL SURFACE - NIR ONLY	20.0	0.0784	0.0604	0.2047	0.0236	0.2494
GRAVEL SURFACE - NIR ONLY	41.0	0.0395	0.0242	0.1942	0.0167	0.1574
GRAVEL SURFACE - NIR ONLY	62.0	0.0171	0.0339	0.1862	0.0189	0.1611
GRAVEL SURFACE - NIR ONLY	64.0	0.0276	0.0299	0.1797	0.0155	0.1664
GRAVEL SURFACE - NIR ONLY	38.0	0.0639	0.0684	0.1805	0.0227	0.1647
GRAVEL SURFACE - NIR ONLY	29.0	0.0950	0.0806	0.1654	0.0222	0.1982

It is interesting to note that the error is often smaller for the sphere model, even though eq. 6 has three parameters and the sphere model has only two. An even better fit is obtained using a similar empirical equation:

$$R = A\theta_v^2 + B\,\theta_v\,[\sin\psi + (\pi-\psi)\cos\psi]/\pi + C \quad . \qquad (7)$$

The coefficients and errors resulting from fitting this equation to the data are given in Tables 5 and 6. Even though this gives a somewhat better fit to the data than eq. 6, the two-parameter spherical model still gives smaller errors in many cases.

Table 5. Coefficients for eq. 7 fit to data from set 1 for rough, medium, and smooth surfaces. Rms errors are also shown.

Surface	ϕ_b(deg)	A	B	C	rms error
ROUGH1	22.5	0.0134	0.1714	0.0558	0.0249
ROUGH2	27.0	-0.0073	0.2001	0.0832	0.0192
ROUGH3	60.0	-0.0437	0.0918	0.1392	0.0121
ROUGH4	70.0	-0.0395	0.0678	0.1293	0.0127
MEDIUM1	47.0	-0.0333	0.1091	0.1058	0.0109
MEDIUM2	62.0	-0.0348	0.0583	0.1304	0.0109
SMOOTH1	46.0	-0.0026	0.0437	0.0661	0.0044
SMOOTH2	52.0	-0.0077	0.0361	0.0742	0.0040

Table 4. Empirical coefficients and errors for non-linear least squares fits of eq. 6 to data from set 2.

Surface and filter	ϕ_b(deg)	A	B	C	rms error
TILLED FIELD - NO FILTER	13.0	0.0049	0.2907	0.1170	0.0305
TILLED FIELD - NO FILTER	22.0	0.0003	0.2754	0.1401	0.0280
TILLED FIELD - NO FILTER	43.0	-0.0472	0.1905	0.1918	0.0198
TILLED FIELD - NO FILTER	65.0	-0.0705	0.1170	0.2330	0.0175
TILLED FIELD - NO FILTER	68.0	-0.0616	0.1182	0.2226	0.0191
TILLED FIELD - NO FILTER	48.0	-0.0448	0.1903	0.1862	0.0184
TILLED FIELD - NO FILTER	38.0	-0.0342	0.2310	0.1773	0.0165
TILLED FIELD - NIR ONLY	13.0	0.0221	0.3402	0.1421	0.0425
TILLED FIELD - NIR ONLY	22.0	0.0102	0.2807	0.1710	0.0336
TILLED FIELD - NIR ONLY	43.0	-0.0469	0.2048	0.2139	0.0256
TILLED FIELD - NIR ONLY	65.0	-0.0584	0.1178	0.2445	0.0207
TILLED FIELD - NIR ONLY	68.0	-0.0584	0.1270	0.2446	0.0187
TILLED FIELD - NIR ONLY	48.0	-0.0401	0.1868	0.2116	0.0194
TILLED FIELD - NIR ONLY	38.0	-0.0353	0.2357	0.2087	0.0186
GRAVEL SURFACE - NO FILTER	12.0	0.0970	0.1588	0.1391	0.0374
GRAVEL SURFACE - NO FILTER	20.0	0.0391	0.1527	0.1975	0.0253
GRAVEL SURFACE - NO FILTER	42.0	0.0152	0.0843	0.2120	0.0164
GRAVEL SURFACE - NO FILTER	62.0	-0.0095	0.0814	0.2102	0.0206
GRAVEL SURFACE - NO FILTER	64.0	0.0116	0.0769	0.1893	0.0238
GRAVEL SURFACE - NO FILTER	38.0	0.0173	0.1540	0.1881	0.0207
GRAVEL SURFACE - NIR ONLY	10.0	0.0626	0.1665	0.1486	0.0307
GRAVEL SURFACE - NIR ONLY	20.0	0.0441	0.1200	0.1906	0.0228
GRAVEL SURFACE - NIR ONLY	41.0	0.0258	0.0478	0.1885	0.0166
GRAVEL SURFACE - NIR ONLY	62.0	-0.0011	0.0634	0.1787	0.0198
GRAVEL SURFACE - NIR ONLY	64.0	0.0104	0.0601	0.1726	0.0150
GRAVEL SURFACE - NIR ONLY	38.0	0.0261	0.1320	0.1650	0.0237
GRAVEL SURFACE - NIR ONLY	29.0	0.0493	0.1594	0.1465	0.0207

LITERATURE CITED

Campbell, G. S. 1981. Fundamentals of radiation and temperature relations. In: Encyclopedia of Plant Physiology. Eds. O. L. Lange, P. S. Nobel, C. B. Osmond, H. Ziegler. Physiological Plant Ecology: Responses to the Physical Environment. Vol. 13A. Springer-Verlag.

Chen, J. 1984. Mathematical Analysis and Simulation in Crop Micrometeorology. Ph.D. Thesis, Agricultural University, Wageningen, The Netherlands.

Egbert, D. D. 1977. A practical method for correcting bidirectional reflectance variations. 1977 Machine Processing of Remot Sensing Data Symposium, Purdue Univ. West Lafayette, IN.

Goel, N. S. and R. L. Thompson. 1984. Inversion of vegetation canopy reflectance models for estimating agronomic variables. III: Estimation using only canopy reflectance data as illustrated by the Suits model. Remote Sensing Environ. 15:223-236.

Norman, J. M., J. M. Welles and E. A. Walter. 1985. Contrasts among bidirectional reflectance of leaves, canopies and soils. IEEE Trans. Geosci. Remote Sens., GE-23:659-667.

Smith, J. A. and K. J. Ranson. 1979. MRS literature survey of bidirectional reflectance and atmospheric corrections, II. Bidirectional reflectance studies literature review. Prepared for NASA/GSFC, 250 pp.

Suits, G. H. 1972. The calculation of directional reflectance of a vegetative canopy. Remote Sens. Environ. 2:117-125.

Walthall, C. L., J. M. Norman, J. M. Welles, G. Campbell, and B. L. Blad. 1985. Simple equation to approximate the bidirectional reflectance of vegetative canopies and bare soil surfaces. 24:383-387.